Quasi-LPV Transformations for Robust Gain Scheduling of Incremental Nonlinear Dynamic Inversion-based Controllers

Pollack, Tijmen; Theodoulis, Spilios; Wang, Xuerui

DOI
10.1016/j.ifacol.2025.10.064

Publication date
2025

Document Version
Final published version

Published in
IFAC-PapersOnline

Available online at www.sciencedirect.com

ScienceDirect

IFAC Papers Online CONFERENCE PAPER ARCHIVE

IFAC PapersOnLine 59-15 (2025) 97–102

Quasi-LPV Transformations for Robust Gain Scheduling of Incremental Nonlinear Dynamic Inversion-based Controllers

Tijmen Pollack * **Spilios Theodoulis** * **Xuerui Wang** *

* *Faculty of Aerospace Engineering, Delft University of Technology, 2629 HS Delft, The Netherlands.*

Abstract: Nonlinear Dynamic Inversion (NDI) has a long and successful history of research and development. The need for gain scheduling for nominal performance may be alleviated with the NDI method, which is accompanied by developmental benefits in terms of design modularity and transparency. However, the robustness of NDI-based control laws remains dependent on the nature of the open-loop plant. In this paper, a design and analysis framework based on quasi Linear Parameter-Varying (q-LPV) system theory is proposed that systematically considers this aspect across nonlinear operating regimes. The q-LPV model framework is presented in the context of robust hybrid incremental NDI control design, which incorporates inversion error compensation in addition to baseline model predictions. Based on a design case study for a simulated aeroservoelastic system, it is shown how systematic gain scheduling of the related inversion compensation design parameters can be performed with the proposed approach.

Keywords: Nonlinear Control, Robust Control, Incremental Nonlinear Dynamic Inversion, Feedback Linearization, quasi-Linear Parameter-Varying Systems, Aeroservoelasticity

1. INTRODUCTION

Nonlinear Dynamic Inversion (NDI) is a celebrated nonlinear control design framework in the flight control community. Some key reasons are its relative conceptual simplicity and the ability it provides to control designers to incorporate well-established LTI design concepts after inversion. NDI also introduces a level of modularity and transparency to the control law, which has significant benefits in different stages of the flight control design process (Pollack (2024)). Consequently, there is a rich history of NDI research and development for aerospace applications.

A subject that continues to attract significant research interest is the robustness of NDI-based control laws. Over time, the question of robust design has led to the use of extended control architectures based on robust outer loop compensators (Adams and Banda (1993)) and *incremental* NDI (INDI) schemes (Wang et al. (2019)). The framework of *hybrid* INDI (Pollack et al. (2024)) is central to the latter category. This approach extends the model-based inversion scheme from basic NDI with an additional inversion error compensation feedback loop that corrects for model prediction errors. The compensation loop can be tuned for predominantly model-based or sensor-based inversion, which results in distinct robustness trade-offs (Pollack and van Kampen (2023)).

In combination with tunable elements in the outer loop, the design parameters associated with this additional compensation can be configured systematically using, for example, H_∞-based synthesis. An important consideration here is the fact that the robustness properties associated with (I)NDI remain dependent on the nature of the open-loop plant. This implies that additional gain scheduling of these parameters may be needed for robustness.

In this paper, the issue of gain scheduling of hybrid INDI compensation parameters for robustness is addressed by establishing a quasi-LPV (q-LPV) model formulation that enables systematic tuning over wide operating regimes. The state transformation method presented by Shamma and Cloutier (1993) forms the basis of the approach. The resulting q-LPV framework is shown to be compatible with the *local linear equivalence* (Leith and Leithead (2000)) principle, which implies that hidden couplings are accounted for (Rugh and Shamma (2000)). It also enables LPV analysis to assess the impact of gain-scheduled inversion compensation on nonlinear stability and performance.

The paper is structured as follows. Section 2 provides a fundamental background on the concepts of (I)NDI and LPV systems. The proposed INDI state transformation q-LPV model is presented in Section 3. The design framework is applied in Section 4 in the context of control of a simulated aeroservoelastic wing section with nonlinearities. Finally, the article is concluded in Section 5.

2. THEORETICAL BACKGROUND

2.1 Incremental Nonlinear Dynamic Inversion

Nonlinear Dynamic Inversion (NDI) follows the principles of classical feedback linearization. To derive an NDI-based control law, it is assumed that the nonlinear open-loop system can be written in an input-affine form as follows:

$$\begin{cases} \dot{\boldsymbol{x}} = \boldsymbol{f}(\boldsymbol{x}) + \boldsymbol{G}(\boldsymbol{x})\boldsymbol{u} \\ \boldsymbol{y} = \boldsymbol{h}(\boldsymbol{x}). \end{cases} \tag{1}$$

10.1016/j.ifacol.2025.10.064

Here, the system description consists of the state vector $\boldsymbol{x} \in \mathbb{R}^n$, the input vector $\boldsymbol{u} \in \mathbb{R}^m$, the controlled variable $\boldsymbol{y} \in \mathbb{R}^m$, and smooth mappings $\boldsymbol{f}$, $\boldsymbol{G}$, and $\boldsymbol{h}$. Input-output linearization with respect to $\boldsymbol{y}$ can be achieved by taking repeated Lie derivatives until the input vector appears:

$$\boldsymbol{y}^{(\boldsymbol{r})} = \begin{bmatrix} \mathcal{L}_f^{r_1} h_1(\boldsymbol{x}) \\ \vdots \\ \mathcal{L}_f^{r_m} h_m(\boldsymbol{x}) \end{bmatrix} + \begin{bmatrix} \mathcal{L}_{g_1}\mathcal{L}_f^{r_1-1} h_1(\boldsymbol{x}) & \dots & \mathcal{L}_{g_m}\mathcal{L}_f^{r_1-1} h_1(\boldsymbol{x}) \\ \vdots & \ddots & \vdots \\ \mathcal{L}_{g_1}\mathcal{L}_f^{r_m-1} h_m(\boldsymbol{x}) & \dots & \mathcal{L}_{g_m}\mathcal{L}_f^{r_m-1} h_m(\boldsymbol{x}) \end{bmatrix} \boldsymbol{u}. \tag{2}$$

which can be written more concisely as:

$$\boldsymbol{y}^{(\boldsymbol{r})} = \boldsymbol{\alpha}(\boldsymbol{x}) + \mathcal{B}(\boldsymbol{x})\boldsymbol{u}. \tag{3}$$

This result can be used to construct a control signal that, under given conditions, cancels all nonlinearities in the output dynamics. When $\hat{\mathcal{B}}$ is invertible, using $\hat{\bullet}$ to denote an estimate and letting $\boldsymbol{\nu}$ represent a known virtual control input, applying the control signal

$$\boldsymbol{u} = \hat{\mathcal{B}}^{-1}(\hat{\boldsymbol{x}}) \left[\boldsymbol{\nu} - \hat{\boldsymbol{\alpha}}(\hat{\boldsymbol{x}}) \right]. \tag{4}$$

will result in a chain of ideal integrators with $\boldsymbol{y}^{(\boldsymbol{r})} = \boldsymbol{\nu}$ in case perfect model and state information is available. For more details, see Khalil (2002).

A key insight is the fact that the nonlinear $\boldsymbol{\alpha}(\boldsymbol{x})$-term can be estimated not only using a model of the mapping of concern, but can also be obtained from the equality in (3):

$$\underbrace{\hat{\boldsymbol{\alpha}}(\hat{\boldsymbol{x}})}_{\hat{\boldsymbol{\xi}}^{MB}} = \underbrace{\boldsymbol{y}^{(\boldsymbol{r})} - \hat{\mathcal{B}}(\hat{\boldsymbol{x}})\boldsymbol{u}}_{\hat{\boldsymbol{\xi}}^{SB}}. \tag{5}$$

This idea can be used for an alternative strategy that is predominantly *sensor-based* (SB). With this approach, specific model information for $\hat{\boldsymbol{\alpha}}(\hat{\boldsymbol{x}})$ is not required. Instead, measurements of $\boldsymbol{y}^{(\boldsymbol{r})}$ and $\boldsymbol{u}$ are used directly. This results in an *incremental* approach to NDI (INDI), where the name stems from the fact that the control law generates incremental inputs $\Delta\boldsymbol{u}$ (Wang et al. (2019)).

The robustness characteristics of a fully sensor-based INDI control law are complementary to those of the classical model-based (MB) variant (Pollack and van Kampen (2023)). Specifically, sensor-based inversion increases robustness to parametric uncertainty associated with $\boldsymbol{\alpha}(\boldsymbol{x})$ at the expense of reduced robustness to high-frequency dynamic uncertainty. Balanced robustness can be obtained by blending both estimates, which is known as the *hybrid* (HB) strategy (Pollack et al. (2024)). This approach actively compensates for model prediction errors by feeding additional sensor-based estimates through a diagonal filter element $H_c \subset \mathcal{RH}_\infty^{n_u \times n_u}$ and compensation gain $K_c \subset \mathcal{R}^{n_u \times n_u}$, where $K_{c_{ij}} \in [0, 1]$. This leads to the scheme:

$$\begin{aligned} \hat{\boldsymbol{\xi}}^{HB} &= (I - K_c H_c)\hat{\boldsymbol{\xi}}^{MB} + K_c H_c \hat{\boldsymbol{\xi}}^{SB} \\ &= \hat{\boldsymbol{\xi}}^{MB} + K_c H_c \boldsymbol{e}_\xi \\ &\triangleq \hat{\boldsymbol{\xi}}^{MB} + K_c \tilde{\boldsymbol{e}}_\xi. \end{aligned} \tag{6}$$

The resulting hybrid INDI control law takes the form of

$$\boldsymbol{u} = \hat{\mathcal{B}}^{-1}(\hat{\boldsymbol{x}}) \left[\boldsymbol{\nu} - \hat{\boldsymbol{\alpha}}(\hat{\boldsymbol{x}}) - K_c \tilde{\boldsymbol{e}}_{\boldsymbol{\xi}} \right]. \tag{7}$$

Here, the *inversion error compensation signal* $K_c \tilde{\boldsymbol{e}}_{\boldsymbol{\xi}}$ corrects for prediction errors $\boldsymbol{e}_\xi = \boldsymbol{\alpha}(\boldsymbol{x}) - \hat{\boldsymbol{\alpha}}(\hat{\boldsymbol{x}})$. To implement this scheme, a scaled complementary filter (SCF) can be used that performs differentiation of the controlled variable at the same time (Pollack et al. (2024)). Note that the control law in (7) is essentially parameter-varying in $\hat{\boldsymbol{x}}$. Accordingly, elements from the LPV framework can be used to systematically tune the corresponding design parameters for robustness over a wide operating domain.

2.2 LPV Systems

Linear Parameter-Varying (LPV) systems form a specific class of systems generally described as:

$$\begin{bmatrix} \dot{\boldsymbol{x}}(t) \\ \boldsymbol{y}(t) \end{bmatrix} = \begin{bmatrix} A(\boldsymbol{\rho}(t)) & B(\boldsymbol{\rho}(t)) \\ C(\boldsymbol{\rho}(t)) & D(\boldsymbol{\rho}(t)) \end{bmatrix} \begin{bmatrix} \boldsymbol{x}(t) \\ \boldsymbol{u}(t) \end{bmatrix}. \tag{8}$$

Here, the state space matrices are functions of a scheduling parameter $\boldsymbol{\rho} \in \mathbb{R}^{n_\rho}$, which is generally time-varying and takes values on a compact set $\mathcal{P} \in \mathbb{R}^{n_\rho}$. The rate of variation $-\beta_i \leq \dot{\rho}_i(t) \leq \beta_i$ may be considered as bounded or unbounded.

Multiple approaches exist to construct state space models that take the form of (8), each with their own advantages and limitations. Some examples include Jacobian linearization, the state transformation method, and the function substitution technique; for more information see, e.g., (Tóth (2010)). The nature of the scheduling parameter forms a distinctive factor here: in case $\boldsymbol{\rho}$ is a function of the system state $\boldsymbol{x}$ or output $\boldsymbol{y}$, the resulting LPV model is referred to as *quasi*-LPV (q-LPV).

Analysis of stability and $\mathcal{L}_2$-performance of LPV systems with bounded rates can be performed based on the Linear Matrix Inequality (LMI) condition from Wu et al. (1996):

$$\begin{bmatrix} \star + X(\boldsymbol{\rho})A(\boldsymbol{\rho}) + \sum_{i=1}^{n_\rho} \beta_i \frac{\partial X}{\partial \rho_i} & X(\boldsymbol{\rho})B(\boldsymbol{\rho}) & C^T(\boldsymbol{\rho}) \\ \star & -\gamma I_{n_u} & D^T(\boldsymbol{\rho}) \\ \star & \star & -\gamma I_{n_y} \end{bmatrix} < 0. \tag{9}$$

Here, the Lyapunov matrix X is described by selected basis functions of $\boldsymbol{\rho}$, allowing for a reduction in the conservativeness of the analysis.

3. INDI-BASED STATE TRANSFORMATION

In this section, a model framework is presented that enables robust gain scheduling of hybrid INDI-based control laws for nonlinear systems that can be described in quasi-LPV form. In particular, the following form presented by Shamma and Cloutier (1993) is considered to this end:

$$\begin{bmatrix} \dot{\boldsymbol{z}} \\ \dot{\boldsymbol{w}} \end{bmatrix} = \begin{bmatrix} k_1(\boldsymbol{z}) \\ k_2(\boldsymbol{z}) \end{bmatrix} + \begin{bmatrix} A_{11}(\boldsymbol{z}) & A_{12}(\boldsymbol{z}) \\ A_{21}(\boldsymbol{z}) & A_{22}(\boldsymbol{z}) \end{bmatrix} \begin{bmatrix} \boldsymbol{z} \\ \boldsymbol{w} \end{bmatrix} + \begin{bmatrix} B_1(\boldsymbol{z}) \\ B_2(\boldsymbol{z}) \end{bmatrix} \boldsymbol{u}. \tag{10}$$

Here, $\boldsymbol{z} \in \mathcal{P}$ is referred to as the scheduling state vector, whereas $\boldsymbol{w}$ represents the remaining non-scheduling states. To arrive at the desired result, the state-transformation approach from Shamma and Cloutier (1993) will be used.

3.1 Augmented NDI Formulation

The framework is presented for the following particular scenario, although extensions to more general cases can be made. First, in accordance with (I)NDI terminology, $\boldsymbol{w}$ is set as the controlled variable and $\boldsymbol{z}$ as the internal state. Moreover, the case where $B_1(\boldsymbol{z}) = 0$ is considered. Application of the inversion law from (4) to this system results in the following closed-loop dynamics:

$$\begin{bmatrix}\dot{\boldsymbol{z}}\\ \dot{\boldsymbol{w}}\end{bmatrix} = \begin{bmatrix}k_1(\boldsymbol{z})\\ 0\end{bmatrix} + \begin{bmatrix}A_{11}(\boldsymbol{z}) & A_{12}(\boldsymbol{z})\\ 0 & 0\end{bmatrix}\begin{bmatrix}\boldsymbol{z}\\ \boldsymbol{w}\end{bmatrix} + \begin{bmatrix}0\\ I\end{bmatrix}\boldsymbol{\nu}. \quad (11)$$

The state-transformation procedure will be followed from hereon; this involves the search for trim maps $\boldsymbol{w}_{eq}$ and $\boldsymbol{\nu}_{eq}$ that satisfy the equilibrium condition

$$\begin{bmatrix}0\\ 0\end{bmatrix} = \begin{bmatrix}k_1(\boldsymbol{z})\\ 0\end{bmatrix} + \begin{bmatrix}A_{11}(\boldsymbol{z}) & A_{12}(\boldsymbol{z})\\ 0 & 0\end{bmatrix}\begin{bmatrix}\boldsymbol{z}\\ \boldsymbol{w}_{eq}\end{bmatrix} + \begin{bmatrix}0\\ I\end{bmatrix}\boldsymbol{\nu}_{eq}. \quad (12)$$

which results in $\boldsymbol{w}_{eq}(\boldsymbol{z}) = -A_{12}^{-1}(\boldsymbol{z})\left(k_1(\boldsymbol{z}) + A_{11}(\boldsymbol{z})\boldsymbol{z}\right)$ and $\boldsymbol{\nu}_{eq} = 0$. Subtracting (12) from (11) yields:

$$\begin{bmatrix}\dot{\boldsymbol{z}}\\ \dot{\boldsymbol{w}}\end{bmatrix} = \begin{bmatrix}0 & A_{12}(\boldsymbol{z})\\ 0 & 0\end{bmatrix}\begin{bmatrix}\boldsymbol{z}\\ \boldsymbol{w} - \boldsymbol{w}_{eq}\end{bmatrix} + \begin{bmatrix}0\\ I\end{bmatrix}\boldsymbol{\nu}. \quad (13)$$

From here, an alternative state-space description can be obtained for the transformed state $\boldsymbol{w}_{dev} \triangleq \boldsymbol{w} - \boldsymbol{w}_{eq}$ by considering its derivative $\frac{\mathrm{d}}{\mathrm{d}t}\boldsymbol{w}_{dev} = \dot{\boldsymbol{w}} - \frac{\partial \boldsymbol{w}_{eq}(\boldsymbol{z})}{\partial z}\dot{\boldsymbol{z}}$; this results in the new formulation:

$$\begin{bmatrix}\dot{\boldsymbol{z}}\\ \dot{\boldsymbol{w}}_{dev}\end{bmatrix} = \begin{bmatrix}0 & A_{12}(\boldsymbol{z})\\ 0 & -\dfrac{\partial \boldsymbol{w}_{eq}(\boldsymbol{z})}{\partial \boldsymbol{z}}A_{12}(\boldsymbol{z})\end{bmatrix}\begin{bmatrix}\boldsymbol{z}\\ \boldsymbol{w}_{dev}\end{bmatrix} + \begin{bmatrix}0\\ I\end{bmatrix}\boldsymbol{\nu}. \quad (14)$$

For meaningful robust design and analysis, the control input $\boldsymbol{u}$ is needed as a performance output. The virtual control $\boldsymbol{\nu}$ does not suffice for this purpose, as it concerns a signal that is internal to the controller itself. Accordingly, $\boldsymbol{u}$ should be incorporated into the transformed q-LPV formulation. To this end, note that the input trim map associated with the inversion law takes the form of:

$$\boldsymbol{u}_{eq}(\boldsymbol{z}) = -B_2^{-1}(\boldsymbol{z})\left(k_2(\boldsymbol{z}) + \begin{bmatrix}A_{21}(\boldsymbol{z}) & A_{22}(\boldsymbol{z})\end{bmatrix}\begin{bmatrix}\boldsymbol{z}\\ \boldsymbol{w}_{eq}(\boldsymbol{z})\end{bmatrix}\right). \quad (15)$$

At this point, we require the q-LPV model to facilitate *Local Linear Equivalence* (LLE) around frozen equilibrium points associated with (12). This property implies that Jacobian linearization of the nonlinear gain-scheduled control system around these points results in equivalent local input-output dynamics (Leith and Leithead (2000)), i.e. without hidden couplings (Rugh and Shamma (2000)). To enable LLE for the input trim map (15), one can augment (14) by considering $\boldsymbol{u}_{eq}(\boldsymbol{z})$ as an extra system state:

$$\begin{bmatrix}\dot{\boldsymbol{z}}\\ \dot{\boldsymbol{w}}_{dev}\\ \dot{\boldsymbol{u}}_{eq}\end{bmatrix} = \begin{bmatrix}0 & A_{12}(\boldsymbol{z}) & 0\\ 0 & -\dfrac{\partial \boldsymbol{w}_{eq}(\boldsymbol{z})}{\partial \boldsymbol{z}}A_{12}(\boldsymbol{z}) & 0\\ 0 & \dfrac{\partial \boldsymbol{u}_{eq}(\boldsymbol{z})}{\partial \boldsymbol{z}}A_{12}(\boldsymbol{z}) & 0\end{bmatrix}\begin{bmatrix}\boldsymbol{z}\\ \boldsymbol{w}_{dev}\\ \boldsymbol{u}_{eq}\end{bmatrix} + \begin{bmatrix}0\\ I\\ 0\end{bmatrix}\boldsymbol{\nu} \quad (16)$$

The complete control input $\boldsymbol{u}$ then follows in accordance with (4) as a performance output:

$$\begin{aligned}\boldsymbol{u} &= B_2^{-1}(\boldsymbol{z})(\boldsymbol{\nu} - A_{22}(\boldsymbol{z})\boldsymbol{w}_{dev}) + \boldsymbol{u}_{eq}\\ &= B_2^{-1}(\boldsymbol{z})(\boldsymbol{\nu} - \boldsymbol{\xi}^{MB}).\end{aligned} \quad (17)$$

The model represented by (16)-(17) is referred to as the *augmented* model-based NDI q-LPV formulation.

3.2 Extension to Inversion Compensation

For hybrid INDI, the q-LPV model must be further extended with inversion compensation elements. To this end, an additional disturbance signal $\boldsymbol{d}_i$ is used to describe bounded model mismatches and external disturbances:

$$\dot{\boldsymbol{w}} = k_2(\boldsymbol{z}) + \begin{bmatrix}A_{21}(\boldsymbol{z}) & A_{22}(\boldsymbol{z})\end{bmatrix}\begin{bmatrix}\boldsymbol{z}\\ \boldsymbol{w}\end{bmatrix} + B_2(\boldsymbol{z})\left(\boldsymbol{u} + \boldsymbol{d}_i\right). \quad (18)$$

With reference to (5), $\boldsymbol{d}_i$ can be observed directly through sensor-based estimation. Therefore, it forms an integral part of the extended q-LPV formulation. Now, in light of (6), the SCF inversion compensation gain $K_c(\boldsymbol{z})$ and filter

$$H_c(\boldsymbol{z}) = \begin{bmatrix}-A_c(\boldsymbol{z}) & A_c(\boldsymbol{z})\\ I & 0\end{bmatrix}. \quad (19)$$

are both set as functions of the scheduling state. This leads to the following *augmented hybrid INDI q-LPV model*:

$$\begin{aligned}\begin{bmatrix}\dot{\boldsymbol{z}}\\ \dot{\boldsymbol{w}}_{dev}\\ \dot{\boldsymbol{u}}_{eq}\\ \dot{\tilde{\boldsymbol{e}}}_{\xi}\end{bmatrix} &= \begin{bmatrix}0 & A_{12}(\boldsymbol{z}) & 0 & 0\\ 0 & -\dfrac{\partial \boldsymbol{w}_{eq}(\boldsymbol{z})}{\partial \boldsymbol{z}}A_{12}(\boldsymbol{z}) & 0 & -K_c(\boldsymbol{z})\\ 0 & \dfrac{\partial \boldsymbol{u}_{eq}(\boldsymbol{z})}{\partial \boldsymbol{z}}A_{12}(\boldsymbol{z}) & 0 & 0\\ 0 & 0 & 0 & -A_c(\boldsymbol{z})\end{bmatrix}\begin{bmatrix}\boldsymbol{z}\\ \boldsymbol{w}_{dev}\\ \boldsymbol{u}_{eq}\\ \tilde{\boldsymbol{e}}_{\xi}\end{bmatrix}\\ &\quad + \begin{bmatrix}0\\ I\\ 0\\ 0\end{bmatrix}\boldsymbol{\nu} + \begin{bmatrix}0\\ B_2(\boldsymbol{z})\\ 0\\ A_c(\boldsymbol{z})B_2(\boldsymbol{z})\end{bmatrix}\boldsymbol{d}_i.\end{aligned} \quad (20)$$

where the control signal now includes the inversion compensation term in accordance with (7):

$$\boldsymbol{u} = B_2^{-1}(\boldsymbol{z})(\boldsymbol{\nu} - \boldsymbol{\xi}^{MB} - K_c(\boldsymbol{z})\tilde{\boldsymbol{e}}_{\xi}). \quad (21)$$

The LLE property is not affected by this formulation, as demonstrated in the following section.

4. CASE STUDY

The proposed hybrid INDI q-LPV model is applied in a case study for control of a nonlinear aeroservoelastic wing section. Note that (I)NDI-based design for control of aeroservoelastic systems has been considered before, as presented by Ko et al. (1997) and Schildkamp et al. (2023).

4.1 Aeroelastic wing section model

The dynamics of the wing section consist in two degrees of freedom, which relate to plunge displacement h and angle-of-attack α. The equations of motion closely follow those described by Sun et al. (2022) and are given as:

$$\begin{aligned}M\begin{bmatrix}\ddot{h}\\ \ddot{\alpha}\end{bmatrix} &= \left(-K(\alpha) + F_x(V_0)\right)\begin{bmatrix}h\\ \alpha - \alpha_g\end{bmatrix}\\ &\quad + \left(-C + F_{\dot{x}}(V_0)\right)\begin{bmatrix}\dot{h}\\ \dot{\alpha} - \dot{\alpha}_g\end{bmatrix} + F_u(V_0)\begin{bmatrix}\beta_1\\ \beta_2\end{bmatrix}.\end{aligned} \quad (22)$$

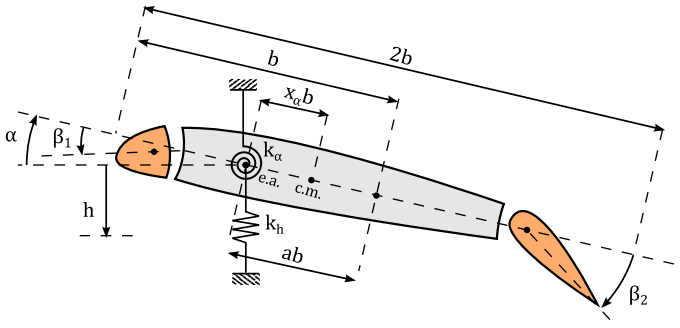

Fig. 1. Nonlinear Aeroelastic Wing Section (illustration based on Lhachemi et al. (2017); Sun et al. (2022))

A scenario in which two control surfaces are available is considered; these are located at the leading and trailing edges respectively, as shown in Figure 1. Both degrees of freedom can be controlled independently with this configuration. The mass M and structural damping C are constant matrices, whereas the structural stiffness matrix is nonlinear according to:

$$K(\alpha) = \begin{bmatrix} k_h & 0 \\ 0 & k_\alpha \left(1 + \delta_{k_\alpha}(\alpha)\right) \end{bmatrix}. \tag{23}$$

Here, δ_{k_α} is a polynomial function of angle-of-attack:

$$\delta_{k_\alpha}(\alpha) = -22.1\alpha + 1315.5\alpha^2 - 8580\alpha^3 + 17289.7\alpha^4. \tag{24}$$

Additionally, the aerodynamic force and moment are modeled in quasi-steady form as follows:

$$F_x(V_0) = \rho V_0^2 b \begin{bmatrix} 0 & c_{L_\alpha} \\ 0 & bc_{m_\alpha} \end{bmatrix}. \tag{25}$$

$$F_{\dot{x}}(V_0) = \rho V_0 b \begin{bmatrix} c_{L_\alpha} & (\frac{1}{2} - a)bc_{L_\alpha} \\ bc_{m_\alpha} & (\frac{1}{2} - a)b^2 c_{m_\alpha} \end{bmatrix}. \tag{26}$$

$$F_u(V_0) = \rho V_0^2 b \begin{bmatrix} c_{L_{\beta_1}} & c_{L_{\beta_2}} \\ bc_{m_{\beta_1}} & bc_{m_{\beta_2}} \end{bmatrix}. \tag{27}$$

Only a single speed $V_0 = 10$ m/s is considered in this case study, whereas the operating region $\mathcal{P}_\alpha$ is limited to ± 10 degrees angle-of-attack. It is assumed that the full system state is available for control purposes. In reality, linear and rotary variable differential transformers can be used.

4.2 Quasi-LPV Hybrid INDI formulation

The hybrid INDI-based control design proceeds as follows. The controlled variable is selected as $\boldsymbol{w} = \begin{bmatrix} \dot{h} & \dot{\alpha} \end{bmatrix}$, while the remaining states $\boldsymbol{z} = [h \ \alpha]$ are considered as scheduling parameters. The virtual control law is selected to generate constant desired modal dynamics across the system's operating range according to:

$$\boldsymbol{\nu} = A_{21}^{(ref)} \boldsymbol{z} + A_{22}^{(ref)} \boldsymbol{w}. \tag{28}$$

Subsequently, the following augmented NDI q-LPV model formulation applies:

$$\begin{bmatrix} \dot{\boldsymbol{z}} \\ \dot{\boldsymbol{w}} \\ \dot{\boldsymbol{u}}_{eq} \end{bmatrix} = \begin{bmatrix} 0 & I & 0 \\ A_{21}^{(ref)} & A_{22}^{(ref)} & 0 \\ 0 & \dfrac{\partial \boldsymbol{u}_{eq}(\boldsymbol{z})}{\partial \boldsymbol{z}} & 0 \end{bmatrix} \begin{bmatrix} \boldsymbol{z} \\ \boldsymbol{w} \\ \boldsymbol{u}_{eq} \end{bmatrix}. \tag{29}$$

where the input trim map gradient follows from:

$$F_u \frac{\partial \boldsymbol{u}_{eq}(\boldsymbol{z})}{\partial \boldsymbol{z}} = \begin{bmatrix} k_h & 0 \\ 0 & k_\alpha \left(1 + \dfrac{\partial \delta_{k_\alpha}(\alpha)\alpha}{\partial \alpha}\right) \end{bmatrix} - F_x. \tag{30}$$

Regarding inversion error compensation, a first-order form is selected for the SCF. The corresponding design parameters are scheduled as a function of α. Consequently, the scheduled hybrid INDI control system is described as:

$$\begin{bmatrix} \dot{\boldsymbol{z}} \\ \dot{\boldsymbol{w}} \\ \dot{\boldsymbol{u}}_{eq} \\ \dot{\tilde{\boldsymbol{e}}}_\xi \end{bmatrix} = \begin{bmatrix} 0 & I & 0 & 0 \\ A_{21}^{(ref)} & A_{22}^{(ref)} & 0 & -K_c(\boldsymbol{z}) I_2 \\ 0 & \dfrac{\partial \boldsymbol{u}_{eq}(\boldsymbol{z})}{\partial \boldsymbol{z}} & 0 & 0 \\ 0 & 0 & 0 & -\tau_c(\boldsymbol{z}) I_2 \end{bmatrix} \begin{bmatrix} \boldsymbol{z} \\ \boldsymbol{w} \\ \boldsymbol{u}_{eq} \\ \tilde{\boldsymbol{e}}_\xi \end{bmatrix} + \begin{bmatrix} 0 \\ F_u \\ 0 \\ \tau_c(\boldsymbol{z}) F_u \end{bmatrix} \boldsymbol{d}_i. \tag{31}$$

where τ_c represents the first-order filter constant.

4.3 Tuning procedure

Thanks to the selected hybrid INDI architecture, the desired nominal modal dynamics are achieved immediately through selection of the virtual control gains:

$$\boldsymbol{\nu} = -\begin{bmatrix} \left(\omega_h^d\right)^2 & 0 & 2\zeta_h^d \omega_h^d & 0 \\ 0 & \left(\omega_\alpha^d\right)^2 & 0 & 2\zeta_\alpha^d \omega_\alpha^d \end{bmatrix} \begin{bmatrix} \boldsymbol{z} \\ \boldsymbol{w} \end{bmatrix}. \tag{32}$$

To improve aeroelastic damping while staying close to the open-loop plant frequency range, the desired modal damping is set to 0.8 while the plunge and pitch frequencies are set to $\omega_h^d = 15$ and $\omega_\alpha^d = 30$ rad/s, respectively. The inversion compensation parameters are synthesized over a grid of LTI systems that results from uniform sampling of (31) over the operating regime. To this end, the following bundled mixed sensitivity synthesis objective is adopted:

$$\begin{bmatrix} \boldsymbol{z}_y \\ \boldsymbol{z}_u \end{bmatrix} = \begin{bmatrix} I & 0 \\ 0 & W_u(j\omega) \end{bmatrix} \begin{bmatrix} S_o G(j\omega) \\ T_i(j\omega) \end{bmatrix} \boldsymbol{d}_i. \tag{33}$$

Minimization of this objective results in balanced performance in terms of input disturbance rejection and robustness to high-frequency unmodeled dynamics. The uncertainty weighting filter $W_u(j\omega)$ is selected to enforce the 0 dB crossover frequency at 300 rad/s. No frequency-dependent shaping is imposed on $S_o G$, for the reason that aeroelastic damping is to be achieved by minimizing the peak gain over all frequencies. In addition, the following constraint is imposed to ensure minimum values for the S-based disk margin (also known as the modulus margin):

$$\left\| S_i(j\omega) \right\|_\infty \leq M_S. \tag{34}$$

In this case study, no further robustness and performance requirements are imposed at the plant output. For a complete design, these should also be incorporated.

Given the structured and multi-tiered nature of the H_∞-synthesis problem, non-smooth optimization techniques are employed. This is achieved with MATLAB® `systune` (Apkarian and Noll (2017)), with (33)-(34) as soft objective and hard constraint, respectively. The resulting gain schedules are presented in Figure 2; here, an increasing sensor-based dependence is shown as $\alpha \to -10$ degrees.

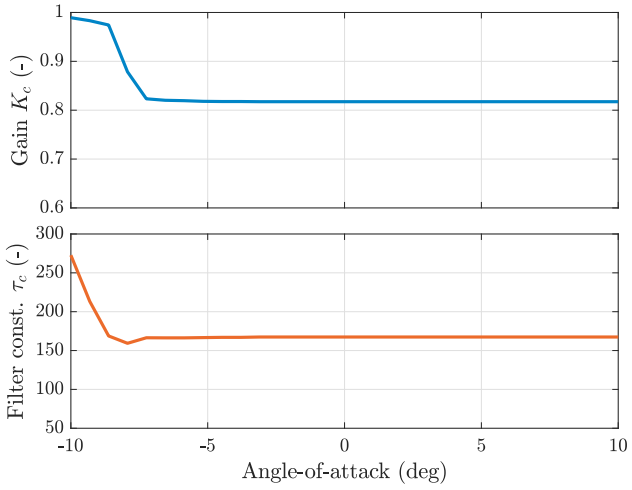

Fig. 2. Scheduled inversion compensation parameters.

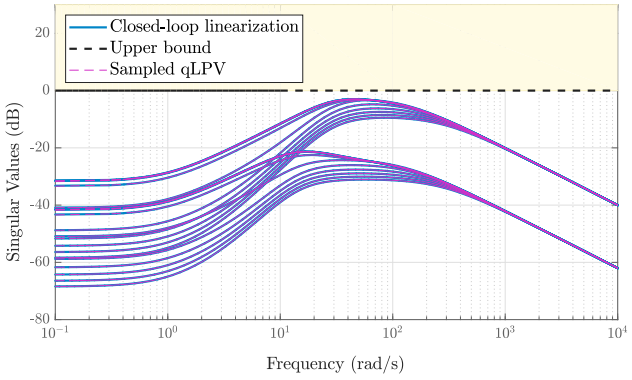

(a) Input disturbance rejection: $S_oG(j\omega)$

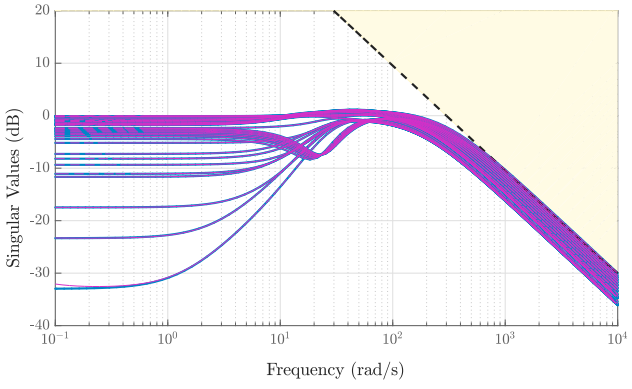

(b) Input complementary sensitivity: $T_i(j\omega)$

Fig. 3. Soft synthesis objectives over selected grid.

4.4 Robustness and LPV performance

Figures 3 and 4 show the frequency responses and weighting templates associated with each of the synthesis objectives. The optimized design meets the robustness objectives in terms of the S-based disk margin and roll-off at high frequencies, whereas the effect of $\boldsymbol{d}_i$ on the system output is attenuated. In addition to direct sampling of the q-LPV model (31), the frequency responses of the system obtained by Jacobian linearization of the closed-loop system have also been visualized. Since the LLE property is satisfied by the q-LPV formulation in (31), the two approaches lead to the same results.

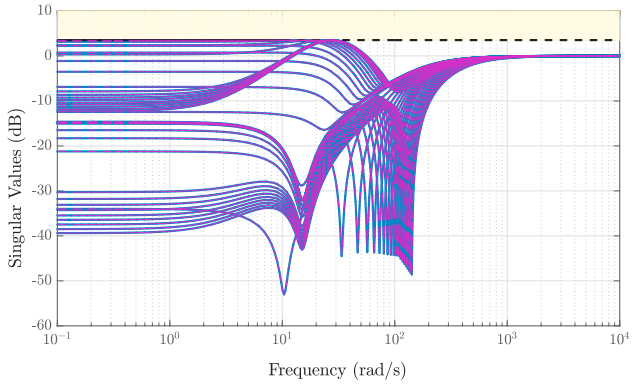

Fig. 4. Hard constraint over selected grid: $S_i(j\omega)$.

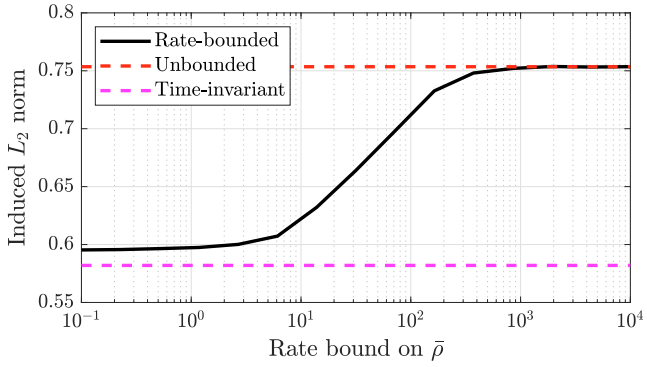

Fig. 5. Input disturbance rejection LPV performance.

With regard to nonlinear stability and performance, the LMI condition from (8) is used to analyze the induced $\mathcal{L}_2$ gain associated with $\boldsymbol{z}_y \leftarrow \boldsymbol{d}_i$ in an LPV context. This is done as a function of angle-of-attack rate bounds. To this end, the nonlinear contribution to the input trim map from (30) is considered in the form of a normalized, lumped scheduling parameter in α:

$$\bar{\rho} \in [0,1] \leftarrow\!\shortmid \frac{\partial \delta_{k_\alpha}(\alpha)\alpha}{\partial \alpha} \quad \text{for} \quad \alpha \in \mathcal{P}_\alpha. \tag{35}$$

Then, the impact of bounded rates $-\beta_i \leq \dot{\bar{\rho}}(t) \leq \beta_i$ is analyzed using a second-order polynomial basis for $X(\bar{\rho})$ over a finite scheduling grid. The `LPVTools` MATLAB® toolbox by (Hjartarson et al. (2015)) is used to this end. The resulting performance levels are plotted in Figure 5. From this result, it is concluded that adequate performance is maintained as $\dot{\alpha} \to \infty$.

4.5 Nonlinear simulation results

Finally, it remains of interest to assess the behavior of the gain-scheduled hybrid INDI control system in a nonlinear simulation scenario. Figure 6 presents the response to non-zero initial conditions under sampled polynomial stiffness uncertainty. In this scenario, the polynomial coefficients in (24) are perturbed randomly by up to ±50% with respect to their nominal values. Also shown in the figure is a comparison to the desired modal dynamics and an illustration of how the closed-loop response is affected if inversion compensation is disabled (i.e., $K_c = 0$). In this case, the design collapses to purely model-based inversion.

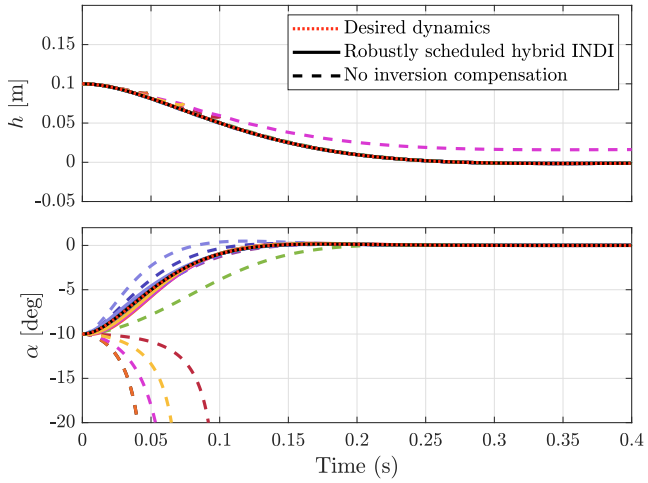

Fig. 6. Nonlinear response under nonzero initial conditions and sampled polynomial stiffness uncertainty.

The simulation results confirm the ability of robustly gain-scheduled hybrid INDI to enhance robustness against nonlinear uncertainty. Without inversion compensation, robust stability is not ensured. At the same time, the nominal modal dynamics are left unaffected. This is despite the additional nonlinearities introduced by the gain-scheduled inversion compensation loop.

5. CONCLUSION

A q-LPV model formulation for hybrid INDI-based controllers has been presented in this paper. With the proposed framework, robust gain scheduling of inversion compensation parameters can be performed systematically for nonlinear systems that can be described in q-LPV form. The framework displays compatibility with the local linear equivalence principle and was used to perform gain scheduling of hybrid INDI parameters for robust control of a nonlinear aeroservoelastic wing section. In this case study, it was shown that robustness was achieved in terms of S-based disk margins and high-frequency uncertainty over the full operating domain. At the same time, the controller could successfully handle nonlinear parametric uncertainties. Moreover, the introduction of extra controller nonlinearities did not affect nominal modal dynamics.

In conclusion, this paper provides valuable insights that enable systematic robust design of hybrid INDI-based controllers over wide operating regimes. In future work, several extensions will be investigated. This includes application to under-actuated systems with many states, discrete-time implementation, and use in LPV synthesis.

REFERENCES

Adams, R. and Banda, S. (1993). Robust flight control design using dynamic inversion and structured singular value synthesis. *IEEE Transactions on Control Systems Technology*, 1(2), 80–92. doi:10.1109/87.238401.

Apkarian, P. and Noll, D. (2017). The H_∞ Control Problem is Solved. *Aerospace Lab*, (13), pages 1–11. doi:10.12762/2017.AL13-01.

Hjartarson, A., Seiler, P., and Packard, A. (2015). LPVTools: A Toolbox for Modeling, Analysis, and Synthesis of Parameter Varying Control Systems. *IFAC-PapersOnLine*, 48(26), 139–145. doi:10.1016/j.ifacol.2015.11.127. 1st IFAC Workshop on Linear Parameter Varying Systems LPVS 2015.

Khalil, H. (2002). *Nonlinear Systems*. Prentice Hall, 3 edition. ISBN 978-0130673893.

Ko, J., Kurdila, A.J., and Strganac, T.W. (1997). Nonlinear Control of a Prototypical Wing Section with Torsional Nonlinearity. *Journal of Guidance, Control, and Dynamics*, 20(6), 1181–1189. doi:10.2514/2.4174.

Leith, D.J. and Leithead, W.E. (2000). Survey of gain-scheduling analysis and design. *International Journal of Control*, 73(11), 1001–1025. doi:10.1080/002071700411304.

Lhachemi, H., Chu, Y., Saussié, D., and Zhu, G. (2017). Flutter suppression for underactuated aeroelastic wing section: Nonlinear gain-scheduling approach. *Journal of Guidance, Control, and Dynamics*, 40(8), 2102–2109. doi:10.2514/1.G002497.

Pollack, T., Theodoulis, S., and van Kampen, E. (2024). Commonalities between robust hybrid incremental nonlinear dynamic inversion and proportional-integral-derivative flight control law design. *Aerospace Science and Technology*, 152, 109377. doi:10.1016/j.ast.2024.109377.

Pollack, T. and van Kampen, E. (2023). Robust Stability and Performance Analysis of Incremental Dynamic-Inversion-Based Flight Control Laws. *Journal of Guidance, Control, and Dynamics*, 46(9), 1785–1798. doi:10.2514/1.G006576.

Pollack, T. (2024). *Advances in Dynamic Inversion-based Flight Control Law Design: Multivariable Analysis and Synthesis of Robust and Multi-Objective Design Solutions*. Dissertation, Delft University of Technology. doi:10.4233/uuid:28617ba0-461d-48ef-8437-de2aa41034ea.

Rugh, W.J. and Shamma, J.S. (2000). Research on gain scheduling. *Automatica*, 36(10), 1401–1425. doi:10.1016/S0005-1098(00)00058-3.

Schildkamp, R., Chang, J., Sodja, J., De Breuker, R., and Wang, X. (2023). Incremental Nonlinear Control for Aeroelastic Wing Load Alleviation and Flutter Suppression. *Actuators*, 12(7). doi:10.3390/act12070280.

Shamma, J.S. and Cloutier, J.R. (1993). Gain-scheduled missile autopilot design using linear parameter varying transformations. *Journal of Guidance, Control, and Dynamics*, 16(2), 256–263. doi:10.2514/3.20997.

Sun, B., Wang, X., and van Kampen, E. (2022). Event-triggered intelligent critic control with input constraints applied to a nonlinear aeroelastic system. *Aerospace Science and Technology*, 120, 107279. doi:10.1016/j.ast.2021.107279.

Tóth, R. (2010). *Modeling and identification of linear parameter-varying systems*. Springer Berlin, Heidelberg. doi:10.1007/978-3-642-13812-6. ISBN 978-3642138126.

Wang, X., van Kampen, E., Chu, Q.P., and Lu, P. (2019). Stability Analysis for Incremental Nonlinear Dynamic Inversion Control. *Journal of Guidance, Control, and Dynamics*, 42(5), 1116–1129. doi:10.2514/1.G003791.

Wu, F., Yang, X.H., Packard, A., and Becker, G. (1996). Induced $\mathcal{L}_2$-norm control for LPV systems with bounded parameter variation rates. *International Journal of Robust and Nonlinear Control*, 6(9-10), 983–998. doi:10.1002/(SICI)1099-1239(199611)6:9/10¡983::AID-RNC263¿3.0.CO;2-C.